On the Theoretical Investigation on Spectroscopy of the Electron Donor−Acceptor Complex TCNE−HMB†

M. Hayashi,‡ T.-S. Yang,‡ J. Yu,‡,§ A. Mebel,‡ and S. H. Lin*,‡,||

Institute of Atomic and Molecular Sciences, Academia Sinica, P. O. Box 23-166, Taipei, Taiwan 106, R.O.C., Department of Chemistry, National Taiwan University, Taipei, Taiwan 106, R.O.C., and Department of Chemistry and Biochemistry, Arizona State University, Tempe, Arizona, 85287-1604

Received: July 2, 1996; In Final Form: April 1, 1997⊗

By performing *ab inito* calculations for the TCNE−HMB complex, we obtain the optimized geometry and the vibrational modes of the ground state. We find that symmetry is broken due to a formation of hydrogen bond between one of the hydrogen atoms of HMB and one of the nitrogen atoms of TCNE. We also find that all the donor−acceptor intermolecular modes are found in the frequency region less than 100 cm^{-1}. We identify donor−acceptor stretching mode at 59 cm^{-1} and two TCNE vibrations at 167 and 170 cm^{-1}, which two modes are highly associated with the experimentally observed mode. Deuteriation effects are also investigated for this complex. We set up a new model for optical transitions, which consists of the two CT states and one ground state including 33 vibrational modes. On the basis of this new model, we analyze the steady state absorption and fluorescence spectra to tentatively obtain potential parameters. We find that the ratio of the transition moment of the CT2 state to that of the CT1 is about 0.3.

1. Introduction

A main feature of electron donor−acceptor (EDA) complex is the appearance of a new absorption band due to the complex formation. Introducing a concept of charge transfer (CT) complex, Mulliken and others reported the pioneering work to explain the mechanism of the new complex formation in solution.[1−4] Later, however, molecular orbital theory allows a more general description of such complex revealing the mechanism of complex formation. It becomes very interesting when either the acceptor or the donor molecule of EDA complex has degenerate orbitals. Mataga and his co-workers, in fact, predicted in their early work on the electron transfer reactions of EDA complexes that, if there are two electron acceptor orbitals originated from an acceptor, it is possible to observe two charge transfer bands when the energy gap of these two orbitals is close.[4] Later, Nagakura *et al.* indeed observed two CT bands of 2,3,5,6-tetracyanobenzene (TCNB), and they concluded that the two CT bands observed in the TCNB complexes are due to the two orbitals of an electron acceptor (TCNB) whose energies are closely located.[4,5]

In the case in which the donor has degenerate orbitals, on the other hand, the CT absorption spectra of such complexes also exhibit multiple peaks. For example, the CT spectra of various complexes of benzene, its aryl derivatives, cycloalkanes, alkenes, and alkynes as donor with TCNE as acceptor were measured, and it is found that some of the CT spectra exhibit two peaks with strongly overlapped features.[6−8] In particular, TCNE−*p*-xylene and TCNE−durene complexes show two partially resolved peaks in the CT spectra. TCNE-alkyl- and alkenylnaphthalenes are also found to exhibit two or three distinctive CT absorbance bands, 550−885 nm, 425−585 nm, and 330−440 nm, and these bands are strongly overlapped.[9]

One of the most interesting EDA complexes is tetracyanoethylene−hexamethylbenzene (TCNE−HMB). Resonance Raman profiles and their analyses on this EDA complex have been reported.[10−15] The weak, far-infrared fluorescence spectrum of this system has also been measured[11,12] by Myers' group. They found the fluorescence spectrum to be narrower than the mirror image of the absorption spectrum. Her group then proposed that the 165 cm^{-1} mode, which they assigned as D-A mode, is not only displaced but also distorted. In addition, the same group showed in their simulation that non-Condon effects make an important contribution to the lower wavenumber edge of the absorption spectrum.

Although the CT spectrum of this complex does not exhibit distinctive multiple peaks, the two closely spaced CT transitions were found on the basis of the quantum chemistry calculation reported by Britt *et al.*[16] The same group also examined the oscillator strengths of the two CT states as a function of several relative geometric configurations at 3.1 Å of TCNE and HMB.[16] They found that for symmetric geometry the transition from the ground state to the CT1 (lower energy CT) state is forbidden, while the oscillator strengths of the CT1 is comparable to that of the CT2 (higher energy CT) state if the less symmetric configurations are chosen.

The major component in the absorption spectrum is the contribution from the CT2 excitation, and the CT1 excitation could contribute to the red side of the absorption band if the symmetric configuration is somehow broken by the interaction with solvent molecules. Aside from the optical transitions, there is the possibility of a nonradiative transition from CT2 to CT1 since there is a small energy difference between the two CT states. This situation allows that CT2 undergoes a faster nonradiative transition compared with the radiative transition from CT2. Thus, it is possible to assume that CT1 is responsible for fluorescence with weaker intensity compared with that of absorption of the two CT transitions. On the basis of this assumption, it becomes important to determine the ratio of the transition dipoles of these CT states.

Moreover, there are some discrepancies in previous studies regarding the spectral modeling and dynamics of this complex. For example, Myers and her co-workers measured absorption, fluorescence, and resonance Raman spectra of TCNE−HMB

† Dedicated to Prof. S. Nagakura on the occasion of his 75th birthday.
‡ Institute of Atomic and Molecular Sciences.
§ Present address: Department of Chemistry, National Kaohsiung Normal University, Kaohsiung, Taiwan, R.O.C.
|| National Taiwan University, Arizona State University.
⊗ Abstract published in *Advance ACS Abstracts,* May 15, 1997.

S1089-5639(96)01973-1 CCC: $14.00

complex in various solvents.[10−12] Estimating resonance Raman cross section and fluorescence cross-section, they found time constants of 1.4−5.9 ps for the back electron transfer from a single CT state to the ground state in CCl_4 solvent.[11] On the other hand, Hochstrasser's group performed femtosecond pump−probe measurements on the same system in both polar and nonpolar solvents. By these direct time-resolved measurements, they observed a back electron transfer rate of $(11.2\ ps)^{-1}$ in the CCl_4 environment.[17]

Myers' group[10] obtained the solvent reorganization energy of about 2 orders of magnitude larger than that predicted by the classical continuum theory. Hochstrasser's group chose 100 cm^{-1} for solvation energy.[17] However, in order to fit the absorption spectrum, they had to assume a large displacement for the electronically excited potential surface along the 165 cm^{-1} mode coordinate and change the 0−0 energy gap from 11 600 cm^{-1}, which was obtained by Myers' group to 13 860 cm^{-1}.[17]

To solve part of these discrepancies, it is necessary to construct a new model that incorporates the two CT states having a small energy gap. This model also allows us to investigate how transient vibrational and vibronic processes lead to back electron transfer after the excitation of one of the CT states. This motivates us to carry out the work presented in this paper.

In this work, we report the results from *ab initio* calculations of the TCNE-HMB complex and discuss important features of the two CT states and show the vibrational modes. Using this model, we analyze the experimental absorption and fluorescence spectra. The paper will be organized as follows. In the next section, we will present our MO calculations and propose a new theoretical model. In section 3, based on our MO results, we will theoretically construct the absorption and fluorescence spectra of TCNE−HMB complex. Our preliminary analysis of the experimental results of the pump−probe experiment reported by Hochstrasser *et al.* is briefly discussed in section 4.

2. *ab Initio* Calculations

Previous experimental study[10−12] has observed a low frequency mode at 165 cm^{-1} and it was tentatively assigned as DA intermolecular stretching vibrational mode.[10] Thus our interest in *ab initio* MO calculation is to obtain the frequency of such a vibrational mode and to investigate other low frequency modes less than 500 cm^{-1}. Using GAUSSIAN 94 program,[18] we perform *ab initio* calculations at the 3-21G level because of the large size of the complex. Understandably, although *ab initio* calculations employing such a small basis set may not give us very accurate results compared with the experimental data, they can still provide a guideline for choosing proper parameters in the theoretical spectral analysis.

We fully optimize the ground state with respect to both inter- and intramolecular degrees of freedom and evaluate vibrational frequencies with the 3-21G basis set. The binding strength of the complex is weak, about 2500 cm^{-1} from the *ab initio* results. From Mulliken analysis, the first and second excited states are confirmed as CT states. Hereafter, we shall define the first and second excited states as CT1 and CT2 states, respectively.

Figure 1 shows the optimized structure of TCNE−HMB complex without solvent molecules. Low symmetry of the optimized structure is the most striking feature of TCNE−HMB complex. This is due to the fact that one hydrogen atom of HMB forms a hydrogen bond with one nitrogen atom of TCNE. This hydrogen bond formation squeezes and attracts the TCNE molecule from any symmetrical positions. This situation can be clearly seen from Figure 1, i.e., the hydrogen bond is formed between the hydrogen and nitrogen atoms at the far left shown in the figure. The distance between these two atoms is about 2.72 Å, while the TCNE−HMB separation, as measured from the center of the HMB ring vertical to the TCNE plane, is about 3.50 Å.

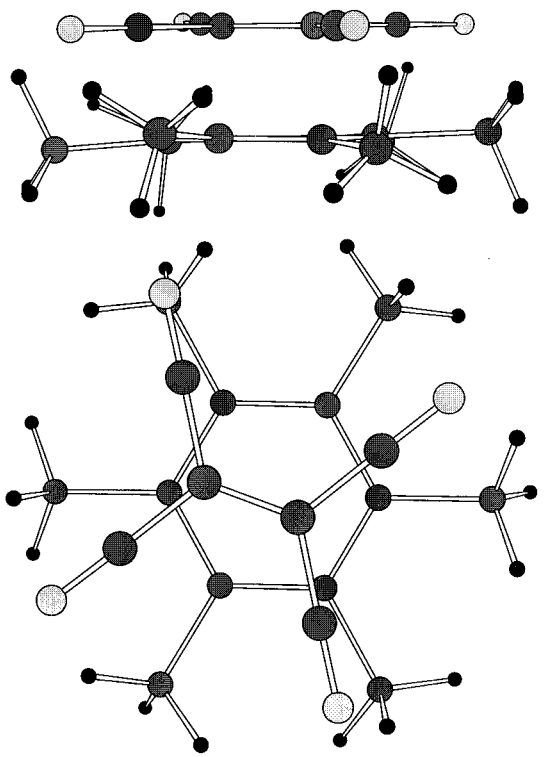

Figure 1. Optimized geometry of TCNE-HMB complex. Note the lower symmetrical geometry of the complex due to the formation of hydrogen bond.

TABLE 1: Frequencies of Benzene Ring Distortion, C═C and C≡N Stretching

calculated[a]	experimental[b]	descriptions
1543 and 1544	1570	HMB ring distortion
1596	1551	TCNE C═C stretching
2313 and 2314	2222	TCNE C≡N stretching

[a] In inverse centimers, scaled by 0.89. [b] In inverse centimers, taken from ref 12.

The TCNE−HMB complex has 114 vibrational modes, of which 24 are TCNE modes and 84 are HMB modes. Thus, ideally, one can identify six intermolecular modes. To compare with the modes found in resonance Raman spectra, we select five frequencies, which show strong Raman activities, from our calculations and list them in Table 1. All calculated frequencies are scaled with a factor of 0.89. These high frequency modes are originated from two benzene ring distortions and one C═C and two motions of C≡N stretching of TCNE.

Table 2 summarizes the frequencies of donor−acceptor vibrational modes whose frequencies are lower than 500 cm^{-1}. We can clearly identify five intermolecular modes of TCNE−HMB complex, while there are two more DA modes highly mixed with a HMB $C-CH_3$ twisting mode. We should note that all DA and DA associated modes (DA/CH_3) are found in the frequency range less than 100 cm^{-1}. We confirm from our *ab initio* calculations and vibrational analysis that the 59 cm^{-1} mode is the DA stretching mode. A HMB $C-CH_3$ twisting mode also couples with several TCNE vibrational modes, creating six complicated modes in the frequency range 100−134 cm^{-1}. We find two HMB modes of 145 and 150 cm^{-1}

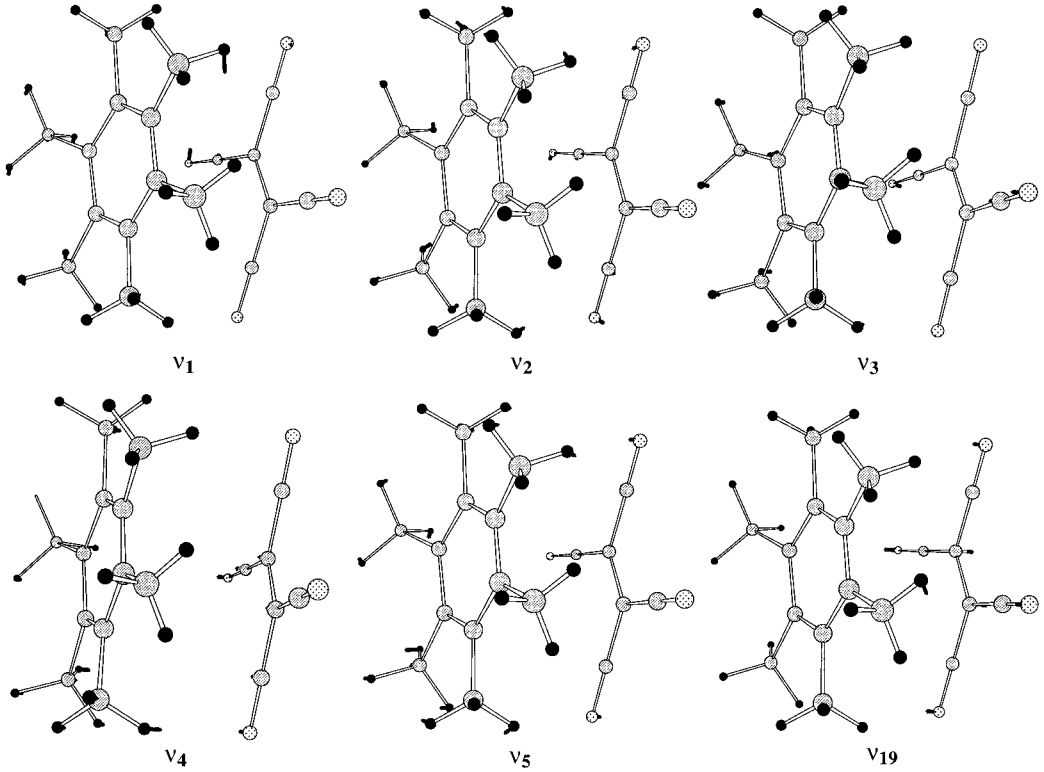

Figure 2. Schematic representation of five DA and TCNE out-of-plane vibration modes of TCNE−HMB complex. ν_1, ν_2, ν_3, ν_4, ν_5, and ν_1 correspond to 9.7, 35, 41, 59, 63, and 170 cm^{-1} modes, respectively.

and two TCNE modes of 167 and 170 cm^{-1}. The 167 and 170 cm^{-1} modes are associated with TCNE C−C≡N bending and out-of-plane vibration, respectively. The 170 cm^{-1} mode is very similar to DA stretching but these two modes are different. Although there is a very small contribution from a HMB C−CH_3 bending mode, the HMB ring carbon atoms do not move rigidly in the 170 cm^{-1} mode. In the DA stretching mode, on the other hand, the TCNE and HMB molecules move collectively. Figure 2 shows the five DA modes indicated by ν_1, ν_2, ν_3, ν_4, and ν_5 corresponding to the 9.7, 35, 41, 59, and 63 cm^{-1} modes, respectively, and the 170 cm^{-1} mode indicated by ν_{19}. Note that all the modes larger than 175 cm^{-1} can be assigned to either HMB or TCNE mode.

The issue as to whether the 165 cm^{-1} mode observed in the experiments[10] is a DA stretching mode or not has drawn considerable attention. From intuitive reasoning, the DA stretching mode involves the motion of CH_3 groups, and hence deuteriation of HMB should induce frequency shift of this mode. However, the experimental study[10,12] did not show deuteriation effects on the observed mode.

Deuteriation, indeed, causes frequency shifts in all of the DA modes in our *ab initio* calculations but the shifts are small ranging from 1.7 to 6.3% changes in their frequencies. In particular, the 59 cm^{-1} mode, the DA stretching mode, shows only 1.7% change. On the other hand, the TCNE out-of-plane vibration mode, whose frequency is very close to that of the observed one, shows no significant deuteriation effect. This situation is consistent with the fact that the HMB mode makes few contribution to the 170 cm^{-1} mode as mentioned above.

One might then conclude that the experimental study[10,12] probably observed the 170 cm^{-1} mode. However, it should also be noted that in our *ab initio* calculations the 167 cm^{-1} mode, TCNE C−C≡N bending, has no deuteriation effect, and this mode has a Raman activity stronger than the 170 cm^{-1} mode. Thus, we do not specifically assign the observed one to the 167 or 170 cm^{-1} mode at present. It will be clarified if the optimized geometries of the two CT states are determined.

TABLE 2: Vibrational Modes with Frequencies Less than 500 cm^{-1}

frequencies[a]	descriptions[b]
9.7 (9.3)	DA twi
35 (33)	DA sli
41 (40)	DA
59 (58)	DA str
63 (59)	DA
72, 79	DA and HMB C−CH_3 twi and ring def
89, 95, 101	HMB C−CH_3 twi and ring def and TCNE C−C≡N out of plane tor
114, 117, 127	HMB C−CH_3 twi and ring def and TCNE C−C≡N ben
132, 134	HMB C−CH_3 twi and ring def and TCNE sci
145, 150	HMB C−CH_3 twi and ring def
167 (167)	HMB C−CH_3 twi and ring def and TCNE C−C≡N ben*
170 (170)	HMB C−CH_3 bend and TCNE out of plane vibration*
175	HMB C−CH_3 bend
207	HMB ring out of plane
291, 305	TCNE
328, 337, 358, 363, 395, 409, 441, 443, 444	HMB

[a] In inverse centimeters, scaled by 0.89 and some of the vibrational frequencies of TCNE-deureriated HMB complex are given in the parentheses. [b] Abbreviations: ben, bending; def, deformation; sci, scissoring; sli, sliding; str, stretch; tor, torsion; twi, twist. [c] The asterisk (*) indicates a major contribution to each mode.

3. Absorption and Fluorescence Spectra

3a. Theory. In this section, we shall analyze absorption and fluorescence spectra of the CT band of the TCNE−HMB complex system theoretically. On the basis of the results obtained in section 2, we consider a model consisting of the

ground state and the CT1 and CT2 states. Absorption occurs from the ground state to the two CT states. CT2 nonradiatively relaxes to CT1 which undergoes a transition to the ground state via both back electron transfer and emission of fluorescence light.

We begin at briefly describing the expressions for absorption and fluorescence spectra, which take into account solvent effects. The absorption coefficient for electronic transitions can be expressed as[19,20]

$$\alpha_{abs}(\omega) \equiv \sum_{s=b,c} \alpha_{as}(\omega)$$

$$= \sum_{s=b,c} \frac{4\pi^2\omega}{3\hbar n_e(\omega)c} \sum_{\{u\}=0}^{\infty} \sum_{\{\upsilon_s\}=0}^{\infty} P_{a\{u\}} |\langle \Theta_{a\{u\}} | \vec{\mu}_{as} | \Theta_{s\{\upsilon_s\}} \rangle|^2 \delta(\omega_{s\{\upsilon_s\},a\{u\}} - \omega) \quad (1)$$

where a, b, and c denote the electronic ground state, CT2 and CT1, respectively. Here $n_e(\omega)$ represents a function of refractive index introduced to correct the static solvent effect, $\{u\}$ and $\{\upsilon_s\}$ are indices for vibrational manifolds of the electronic ground state and the CT states, respectively, $P_{a\{u\}}$ is the Boltzmann distribution function for the population in the manifold $\{au\}$, $\vec{\mu}_{as}$ is the electronic transition moment, $\Theta_{b\{\upsilon_s\}}$, for example, depicts the multimode nuclear wave function of CT states, and finally $\hbar\omega_{s\{u_s\},a\{u\}}$ denotes the energy gap between the vibronic states $s\{\upsilon_s\}$ and $a\{u\}$.

Equation 1 can be expressed in terms of N nuclear correlation functions. Notice that the motions of some DA modes are subject to the dynamical interactions with solvent molecules. To include the solvent effects, we derive nuclear correlation functions for relevant DA and DA/CH_3 modes by solving the Langevin equation of a damped oscillator. In describing the system vibrational motions by N harmonic oscillators, we divide the N nuclear correlation functions into two parts; the DA and DA/CH_3 modes which couple with solvent are denoted by N_{low} and the rest of the vibrational modes by N_{high}. Under the Condon approximation, the absorption cross-section then is rewritten as

$$\alpha_{ab}(\omega) = \frac{4\pi\omega}{3\hbar n_e(\omega)c} |\vec{\mu}_{ab}|^2 \mathrm{Re} \int_0^\infty dt \exp\{it(\omega - \omega_{ba})\} \times \prod_{i=1}^{N_{low}} G^i_{ba}(t) \prod_{j=1}^{N_{high}} G^j_{ba}(t) \quad (2)$$

Here $G^i_{ba}(t)$ represents the nuclear correlation function of the DA modes which couple with solvent and is given by[21]

$$G^i_{ba}(t) = \exp[\gamma^i_{ba}(t)] \quad (3)$$

with

$$\gamma^i_{ba}(t) = -itS_i\omega_i - \frac{d_i^2 kT}{\hbar^2}\left[\gamma t + \{e^{-\gamma t/2}\cos(\omega_1 t) - 1\} \times \frac{(\gamma^2 - \omega_i^2)}{\omega_i^2} + e^{-\gamma t/2}\sin(\omega_1 t)\frac{(\gamma^2 - 3\omega_i^2)\gamma}{2\omega_1\omega_i^2}\right] \quad (4)$$

where

$$\omega_1^2 = \omega_i^2 - (\gamma/2)^2 \quad (5)$$

and $S_i = (\omega_i/2\hbar)d_i^2$ (d_i = the potential displacement along the coordinate Q_i) is the Huang−Rhys factor, and γ is the friction coefficient. The thermal average over the initial vibrational states and the statistical average over solvent interactions have been carried out using the cumulant expansion method.[21,22] Under the Stokes law, γ can be evaluated from solvent viscosity. In the case of an underdamped oscillator, $\omega_i \gg \gamma$, eq 4 reduces to

$$\gamma^i_{ba}(t) = -itS_i\omega_i - \frac{2S_i kT}{\hbar\omega_i}\{\gamma t - e^{-\gamma t/2}\cos(\omega_i t) + 1\} \quad (6)$$

The rest of the vibrational modes of the DA complex are treated as the displaced harmonic oscillators quantum mechanically. Their nuclear correlation functions can be written as[19]

$$G^j_{ba}(t) = \exp[S_j\{(\bar{n}_j + 1)(e^{-it\omega_j} - 1) + \bar{n}_j(e^{it\omega_j} - 1)\}] \quad (7)$$

The final expression for the absorption coefficient is given by

$$\alpha_{ab}(\omega) = \frac{4\pi\omega}{3\hbar n_e(\omega)c} |\vec{\mu}_{ab}|^2 \mathrm{Re} \int_0^\infty dt \exp\{it(\omega - \omega_{ba})\} \exp\left[\sum_{j=1}^{N_{high}} S_j\{(\bar{n}_j + 1)(e^{-it\omega_j} - 1) + \bar{n}_j(e^{it\omega_j} - 1)\} + \sum_{i=1}^{N_{low}} \gamma^i_{ba}(t)\right] \quad (8)$$

$\alpha_{ac}(\omega)$ can be derived in the same fashion as well.

Similarly, the fluorescence spectrum for the electronic transition c → a in the adiabatic approximation is given by[19]

$$I_{ca}(\omega) = \frac{4n_e(\omega)\omega^3}{3c^3 A_{ca}} |\vec{\mu}_{ca}|^2 \mathrm{Re} \int_0^\infty dt \exp\{it(-\omega + \omega_{ca})\} \times \exp\left[\sum_{j=1}^{N_{high}} S_j\{(\bar{n}_j + 1)(e^{-it\omega_j} - 1) + \bar{n}_j(e^{it\omega_j} - 1)\} + \sum_{i=1}^{N_{low}} \gamma^i_{ca}(t)\right] \quad (9)$$

where A_{ca} represents the radiative rate constant.

3b. Spectral Analysis and Molecular Parameters. We shall analyze the absorption and fluorescence spectra of TCNE−HMB complex in CCl_4 solvent at 293 K.[12] For this purpose, we need values for the molecular variables such as vibrational frequency ω_j, Huang−Rhys factors S_j of the two CT states, the ratio of the two transition moments of CT1 and CT2, $|\vec{\mu}_{ca}|/|\vec{\mu}_{ba}|$, the energy difference between CT1 and CT2, and the electronic transition energy between CT2 and the ground state $\hbar\omega_{ba}$.

First we consider all the modes found in our *ab initio* calculations with vibrational frequencies smaller than 310 cm^{-1}. For simplicity, we divide these modes into three groups on the basis of the nature of each mode. We obtain: (1) five DA and two DA/CH_3 modes; (2) 14 HMB and/or TCNE modes with energy larger than 80 cm^{-1} but less than the thermal energy of room temperature; and (3) 2 TCNE modes smaller than 310 cm^{-1}.

The Huang−Rhys factors for the group 1 are associated with the imaginary part of eq 6, i.e., an energy shift due to the interaction with solvent. We set the Huang−Rhys factors for those modes of CT1 such that the energy shift equals to 50 cm^{-1}. The friction coefficient, γ, in eq 6 was estimated by employing the Stokes model consisting of a geometrical factor of 4 Å, a mass of 4.8×10^{-25} kg, and a viscosity of 0.97 mPa s for the CCl_4 solvent.[23] We have also performed numerical calculations using geometrical factor values other than but nearby 4 and found that the spectral analysis is insensitive to this change.

TABLE 3: Molecular Parameters for the Absorption and Fluorescence Bands of the CT States of TCNE−HMB Complex in CCl_4 Solvent

number of modes	description	frequencies	$\|\Delta Q\|$ CT1/CT2	
7	DA/CH_3 modes	51.2[b]	0.54	0.66[f]
14	TCNE and/or HMB	137[c]	1.28	1.57[f]
2	TCNE	298[d]	0.42	0.52[f]
1	HMB[d]	450[e]	1.33[e]	1.63[f]
1	TCNE[d]	542[e]	0.52[e]	0.64[f]
1	TCNE[d]	600[e]	0.54[e]	0.66[f]
1	HMB[d]	968[e]	0.44[e]	0.54[f]
1	HMB[d]	1292[e]	0.60[e]	0.74[f]
1	HMB[d]	1386[e]	0.30[e]	0.36[f]
1	HMB[d]	1437[e]	0.23[e]	0.28[f]
1	TCNE[d]	1551[e]	0.88[e]	1.08[f]
1	HMB[d]	1570[e]	0.29[e]	0.36[f]
1	TCNE[d]	2222[e]	0.44[e]	0.54[f]

[a] In inverse centimeters. [b] The 5 DA and 2 DA/CH_3 modes listed in Table 2 are averaged. [c] The 14 TCNE and/or HMB modes ranging from 80 to 210 cm^{-1} listed in Table 2 are averaged. [d] The 2 TCNB modes of 327 and 343 cm^{-1} listed in Table 2 are averaged. [e] Those parameters are employed from ref 12; $\hbar\omega_{ca} = 13\,910$ cm^{-1}, $\hbar\gamma = 4.5$ cm^{-1} (for the viscosity relaxation rate constant), $T = 293$ K. [f] Those parameters are obtained by increasing each ΔQ of CT1 by 23%; $\hbar\omega_{ba} = 14\,310$ cm^{-1}

Next, for the modes of CT1 with energies higher than 310 cm^{-1}, we adopt the Huang−Rhys factors determined by Myers *et al.* via the resonance Raman and fluorescence spectra.[12] The transition frequency and $|\Delta Q|$ for the 137 and 298 cm^{-1} modes can be obtained by analyzing the fluorescence spectrum. We thus analyze the fluorescence spectrum based on eq 9 and find that 13 910 cm^{-1} is an appropriate electronic transition energy and the best fit is obtained when $|\Delta Q|$ for the 137 and 298 cm^{-1} modes are set to be 1.28 and 0.42, respectively. We should note that the Huang−Rhys factor for the group (2) of CT2 plays a very important role in the quantum beat appearing in the time-resolved profile reported by Hochstrasser's group since the dominant beat frequency corresponds to one of these modes.

To analyze the absorption spectra, for the Huang−Rhys factors of the modes of CT2 with energies higher than 310 cm^{-1}, we increase the displacements of CT1 by 23%, which was suggested by Hochstrasser's group[17] who increased the displacements of Myers' group[10] by 23% to obtain the best fit of the observed absorption spectra. We assume that the displacements of all the groups of CT2 are obtained by increasing the corresponding displacements of CT1 by 23%.

To obtain the energy gap between the two CT states, we have performed semiempirical MO calculations based on INDO/S.[36] Our semiempirical MO calculations suggest 400 cm^{-1} for the energy gap between the CT1 and CT2 states. Thus, the electronic transition energy between the electronic ground state and CT2 is given by 14 310 cm^{-1}. Table 3 summarizes the numbers for the molecular variables of both CT1 and CT2. By fitting CT1 and CT2 absorption bands to the observed absorption spectrum, we find the best ratio is about 0.3 for $|\vec{\mu}_{cg}|/|\vec{\mu}_{bg}|$.

Since the absorption coefficients are not available to us, the magnitudes of $|\vec{\mu}_{bg}|$ and $|\vec{\mu}_{cg}|$ cannot be determined.

Figure 3 demonstrates the calculated fluorescence and absorption spectra, and for comparison we also superimpose the experimental data reported by Myers' group.[12] We decompose the absorption band into two CT bands and the result is shown in Figure 4. Although in our calculation we do not consider the coordinate dependence of the electronic transition moment (i.e., the non-Condon effect) and the distortion of the potential surfaces for the normal modes, our simulation shows

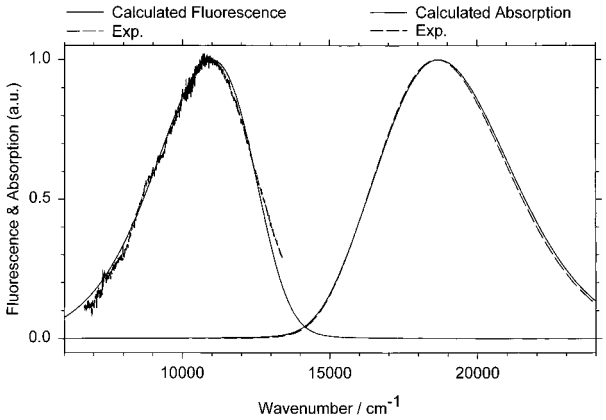

Figure 3. Simulation of the absorption and fluorescence spectra of the CT1 and CT2 bands of the TCNE−HMB complex in the CCl_4 solvent at 293 K.

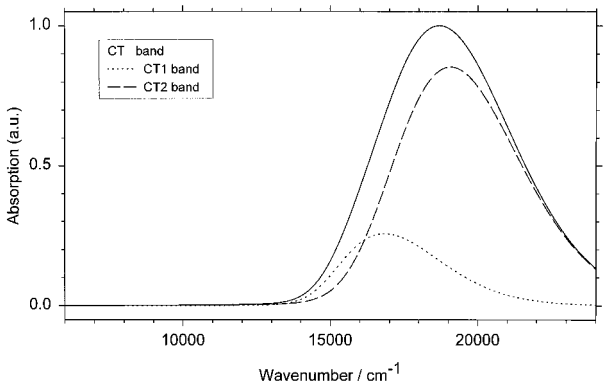

Figure 4. Simulation of the CT1 and CT2 absorption bands of the TCNE−HMB complex in the CCl_4 solvent at 293 K.

good agreement with the experimental data. It should be noted that if we use for the CT2 band the same $|\Delta Q|$ values as obtained from the CT1 band, there are considerable deviations at high energy band side of the observed CT absorption spectrum.

Having employed a number of assumptions for obtaining the $|\Delta Q|$ values, we should note that these values are tentatively but reasonably assigned. However, individual $|\Delta Q|$ value for each mode can also be obtained if the optimized geometries of the two CT states are determined by *ab initio* calculations.

4. Discussion and Conclusion

We have analyzed femtosecond pump−probe profiles of the TCNE−HMB complex in the CCl_4 solvent reported by Hochstrasser's group on the basis of a single mode model. Although there are a number of vibrational modes observed in the optical spectra, we assume that only the 137 cm^{-1} mode of the group 1, which is associated with the 165 cm^{-1} mode and the 161.7 cm^{-1} mode reported by Myers' group and Hochstrasser's group, respectively, plays a dominant role in transient behaviors such as quantum beats and nonradiative transition from the CT2 to CT1 surfaces. This assumption allows us to roughly estimate the vibrational relaxation and dephasing rate constant for the CT1 and CT2 states. By solving the coupled master equations for the vibrational and vibronic dynamics,[24−31] we find that the vibrational relaxation and pure dephasing take place at the rates of 2.5 and 0.5 ps^{-1}, respectively, and that the back electron transfer process has a time constant of 11.2 ps.

These results suggest that the back electron transfer takes place after the system achieves vibrational equilibrium, and we can regard the back electron transfer process as internal conversion. In the case of single promoting mode, the rate

constant of internal conversion (IC) is given by[32]

$$W(\mathrm{c} \rightarrow \mathrm{a}) = |\frac{R^l_{\mathrm{ac}}}{\hbar}|^2\left(\frac{\omega_l}{2\hbar}\right)\mathrm{Re}\int_0^\infty \mathrm{d}t\, \exp\{it(\omega_{\mathrm{ac}} + \omega_l)\} \times \prod_{j=1}^{N_{\mathrm{high}}} G^j_{\mathrm{ac}}(t) \prod_{i=1}^{N_{\mathrm{low}}} G^i_{\mathrm{ac}}(t) \quad (10)$$

where $R^l_{\mathrm{ac}} = -\hbar^2\langle\Phi_{\mathrm{a}}|\partial/\partial Q_l|\Phi_c\rangle$ is an electronic coupling matrix element. Equation 10 can be written in the Fermi golden form as

$$W(\mathrm{c} \rightarrow \mathrm{a}) = \frac{2\pi}{\hbar}|V_{\mathrm{ca}}|^2\sum_u\sum_w P_{\mathrm{a}\{u\}}|\langle\Theta_{\mathrm{a}\{u\}}|\Theta_{\mathrm{c}\{w\}}\rangle|^2 \times \delta(E_{\mathrm{a}\{u\}} - E_{\mathrm{c}\{w\}} + \hbar\omega_l) \quad (11)$$

where V_{ca} denotes the electronic coupling matrix element of IC[32] and is given by $V_{\mathrm{ca}} = R^l_{\mathrm{ac}}(\omega_l/2\hbar)^{1/2}$. Given $W(\mathrm{c} \rightarrow \mathrm{a}) = 0.0892\ \mathrm{ps}^{-1}$ [17] and employing all the values for the CT1 state listed Table 3, we find the electronic coupling constant, $R^l_{\mathrm{ac}}(\omega_l/2\hbar)^{1/2}$, to be 310 cm^{-1}.

We also investigate the temperature dependence of the IC rate constant. We find that the IC rate constant does not show any significant temperature dependence for temperatures ranging from 250 to 330 K. This situation is quite understandable since the energy gap between CT1 and the ground states is 13 910 cm^{-1} and we assumed that the promoting mode is a high frequency mode so that $\bar{n}_l \approx 0$ in this temperature range. In other words, the integral part of the eq 10 is independent of temperature for the TCNE−HMB in CCl_4 solvent in the temperature range under consideration. We also investigate solvent effects on the temperature dependence of the IC rate constant by changing the viscosity relaxation constant but holding $\hbar\omega_i \gg \hbar\gamma$. When we increase $\hbar\gamma$ by a factor of 2.3, the IC rate constant shows a very small increase of 0.44% as the temperature goes from 250 to 330 K.

We should note that some of the CT spectra of various complexes of benzene, its aryl derivatives, cycloalkanes, alkenes, and alkynes as donor with TCNE as acceptor were reported to exhibit two peaks with strongly overlapped features.[6−8] TCNE−alkyl- and alkenylnaphthalenes were found to exhibit two or three CT absorbance bands 550−885, 425−585, and 330−440 nm.[9] Although the peaks are well-resolved, the bands are also strongly overlapped. It is thus interesting to investigate the dynamics of these systems experimentally.

Although we do not discuss the multimode effects on the transient dynamics, it should be investigated in the future. The multimode effects can be observed when shorter laser pulses are used experimentally.

In conclusion, based on the results of molecular orbital calculations, we have proposed a new theoretical model for both spectral features and ultrafast dynamics of the TCNE−HMB complex consisting of two CT states. We have performed MO calculations employing GAUSSIAN94. We have found that the symmetry is broken in the optimized ground state structure obtained from the GAUSSIAN94 calculations. This symmetry-broken structure is due to a formation of hydrogen bond between one of the hydrogen atoms and one of the nitrogen atoms. The GAUSSIAN94 calculations also suggest a number of low-frequency vibrational modes in the ground state. However, all DA and DA/CH_3 modes are found in the vibrational frequency region smaller than 100 cm^{-1}. Recently, fully optimized ground state calculations have been performed on the benzene−TCNE[33] complex at the HF/6-311G** level with GAUSSIAN 90 by Cioslowski. In this case, the symmetrical structure was found in the optimized geometry. He found that the buckling of the TCNE moiety makes a significant contribution to the dipole moment. Using a smaller basis set in this work we also produce the buckling of TCNE.

On the basis of MO calculations and the fluorescence and resonance Raman measurements reported by Myers' group, we construct a model which consists of two CT states and 33 active vibrational modes, seven of which modes are associated with DA or DA/CH_3 modes subject to the interaction with solvent. We assume that all the vibrational modes in our model are displaced harmonic oscillators. By taking into account solvent interaction effects via viscosity and employing the parameters for high-frequency modes due to Myers' group, we analyze the fluorescence spectrum of the TCNE−HMB CT1 band. We find that the energy gap between CT1 and the ground states is 13 910 cm^{-1}. This allows us to investigate the molecular variables for CT2 by simulating the absorption spectra. We estimate that the CT1 absorption band contributes only a factor of 0.3 to the total CT band.

The experimentally observed CT spectra of TCNE−alkylbenzene complexes, depending on their donor molecules, were found to be well-represented by either an asymmetric Gaussian function or two asymmetric Gaussian functions.[7] For example, TCNE−*p*-xylene and TCNE−durene complexes show two partially resolved peaks in the CT spectra. If the transition frequencies of the two CT states are separated larger than 1400 cm^{-1}, the absorption spectra are well-decomposed into two asymmetric Gaussian functions. In this case, the ratio of the fitted peak intensity of the higher state to that of the lower state varies 0.77−1.61, which is approximately associated with the oscillator strength ratios. For the TCNE−HMB system, two peaks are not resolved. This might be due to the fact that the energy gap between the two CT states are only several hundred wavenumbers and the intensity ratio is small. For a better understanding of the transition moments of the two CT states, one should explore the excited state properties such as potential surfaces and transition moments as a function of vibrational coordinates. However, very consistent and accurate theoretical methods are needed, which are not available at present. It should be noted that some effects have been examined by McHale's group to partially overcome the difficulty. Recently, they have combined *ab initio* and semiempirical methods to investigate TCNE−indene[34] and TCNE−benzene complexes.[35] They obtained the geometrical conformations and intermolecular potentials of those electronic ground states and the energies and the oscillator strengths of the two CT states as a function of energetically accessible conformations.

We use 50 cm^{-1} for the energy shift due to the group 1 modes via the interaction with solvent. It is not necessary to introduce solvent reorganization energy in the present case if one takes into account all the possible inter- and intravibrational modes in the electronic transition. Britt *et al.* have pointed out that the applicability of dielectric continuum theories to account for the solvent reorganization energy should be examined.[16] They also suggested a possible contribution of inter- and intramolecular vibrational modes to the electronic transition. It should be noted that a more detailed microscopic theory should be developed for a better understanding of the nature of the interaction between CT complex and solvent.

Acknowledgment. This work was supported by the National Science Council of the Republic of China. We would like to thank Prof. Anne B. Myers for providing us her absorption and

fluorescence spectra. We also would like to thank the referees for their useful comments and suggestions.

References and Notes

(1) Mulliken R. S.; Person, W. B. *Molecular Complexes*, Wiley: New York, 1969.

(2) Briegleb, G. *Elektronen-Donator-Accpetor-Komplexe*, Springer-Verlag: Berlin, 1961; p 50.

(3) Voigt, E. M. *J. Am. Chem. Soc*. **1964**, *86*, 3611.

(4) Mataga N.; Kubota, T. *Molecular Interactions and Electronic Spectra*, Marcel Dekker: New York, 1970.

(5) Iwata, S.; Tanaka, J.; Nagakura, *J. Am. Chem. Soc.* **1966**, *88*, 894.

(6) Michaelian, K. H.; Rieckhoff, K. E.; Voigt, E. M. *Proc. Natl. Acad. Sci. U.S.A.* **1975**, *72*, 4196.

(7) Rossi, M.; Buser, U.; Haselbach, E. *Helv. Chim. Acta* **1976**, *59*, 1039.

(8) Frey, J. E.; Andrews, A. M.; Ankoviac, D. G.; Beaman D. N.; Du Pont, L. E.; Elsner, T. E.; Lang, S. R.; Oosterbaan Zwart, M. A.; Seagle, R. E.; Torreano, L. A. *J. Org. Chem*. **1990**, *55*, 606.

(9) Frey, J. E.; Andrews, A. M.; Combs, S. D.; Edens, S. P.; Puckett, J. P.; Seagle, R. E.; Torreano L. A. *J. Org. Chem*. **1992**, *57*, 6462.

(10) Markel, F.; Ferris, N. S.; Gould, I. R.; Myers, A. B. *J. Am. Chem. Soc.* **1992**, *114*, 6208.

(11) Kulinowski, K.; Gould, I. R.; Myers, A. B. *J. Phys. Chem.* **1995**, *99*, 9017.

(12) Kulinowski, K; Gould I. R.; Ferris N. S.; Myers A. B. *J. Phys. Chem*. **1995**, *99*, 17715.

(13) Britt, B. M.; Lueck, H. B.; McHale, J. L. *Chem. Phys. Lett*. **1992**, *190*, 528.

(14) Smith, M. L.; McHale, J. L. *J. Phys. Chem.* **1985**, *89*, 4002.

(15) Mchale, J. L.; Merriam, M. J. *J. Phys. Chem.* **1989**, *93*, 526.

(16) Britt, B. M.; McHale, J. L.; Friedrich D. M. *J. Phys. Chem.* **1995**, *99*, 6347.

(17) Wynne, K.; Gralli, C.; Hochstrasser R. M. *J. Chem. Phys.* **1994**, *100*, 4707.

(18) Frisch, M. J.; Trucks, G. W.; Schlegel, H. B.; Gill, P. M. W.; Johnson, B. G.; Robb, M. A.; Cheeseman, J. R.; Keith, T.; Petersson, G. A.; Montgomery, J. A.; Raghavachari, K.; Al-Laham, M. A.; Zakrzewski, V. G.; Ortiz, J. V.; Foresman, J. B.; Cioslowski, J.; Stefanov, B. B.; Nanayakkra, A.; Challacmbe, M.; Peng, C. Y.; Ayala, P. Y.; Chen, W.; Wong, M. W.; Andres, J. L.; Binkley, J. S.; Defrees, D. J.; Baker, J.; Stewart, J. P.; Head-Gordon, M.; Gonzalez, C.; Pople, J. A. *Gaussian 94*, Revision B.2, Gaussian Inc.: Pittsburgh, PA, 1995.

(19) Eyring, H.; Lin, S. H.; Lin, S. M. *Basic Chemical Kinetics*, Weily-Interscience: New York, 1980.

(20) Kono, H.; Ziv, A. R.; Lin, S. H. *Surf. Sci.* **1983**, *134*, 614.

(21) Villaeys, A. A.; Boeglin, A.; Lin, S. H. *J. Chem. Phys.* **1985**, *82*, 4044.

(22) Kubo, R. *J. Phys. Soc. Jpn.* **1962**, *17*, 1100.

(23) *Handbook of Chemistry and Physics*, 71th ed., CRC: Boca Raton, 1990.

(24) Fan, B.; Lin, S. H.; Hamer, N. *J. Chem. Phys.* **1989**, *91*, 4485.

(25) Lin, S. H.; Fan, B.; Hamer, N. *Adv. Chem. Phys.* **1990**, *79*, 133.

(26) Lin, S. H.; Alden, A.; Islampour, R.; Ma, H.; Villaeys, A. A. *Density Matrix Method and Femtosecond Processes*, World Scientific: Singapore, 1991.

(27) Suzuki, S.; Sung, H. C.; Hayashi, M.; Lin, S. H. *Physica A* **1995**, *221*, 15.

(28) Sugawara, M.; Fujimura, Y.; Yen, C. Y.; Lin, S. H. *J. Photochem. Photobiol*. **1990**, *A54*, 321.

(29) Gu, X. Z.; Hayashi, M.; Suzuki, S.; Lin, S. H. *Biochim. Biophys. Acta* **1995**, *1229*, 215.

(30) Sugawara, M.; Hayashi, M.; Suzuki, S.; Lin, S. H. *Mol. Phys.* **1996**, *87*, 637.

(31) Lin, S. H. *J. Chem. Phys.* **1974**, *61*, 3810.

(32) Lin, S. H. *J. Chem. Phys.* **1966**, *44*, 3759.

(33) Cioslowski, J. *Int. J. Quantum Chem*. **1994**, *49*, 463.

(34) Edwards, W. D.; Du, M.; Royal, J. S.; McHale, J. L. *J. Phys. Chem.* **1990**, *94*, 5748.

(35) Emery, L. C.; Sheldon, J. M.; Edwards, W. D.; McHale, J. L. *Spectrochim. Acta* **1992**, *48A*, 715.

(36) Ridley, J.; Zerner, M. C. *Theor. Chim. Acta* **1973**, *32*, 111; **1976**, *42*, 323.